Electronic Supplementary Material (ESI) for ChemComm.

Electronic Supplementary Information (ESI)

Efficient charge separation on 3D architectures of TiO_2 mesocrystals packed with chemically exfoliated MoS_2 shell in synergetic hydrogen evolution

Peng Zhang,[a] Takashi Tachikawa,[b]* Mamoru Fujitsuka[a] and Tetsuro Majima[a]*

[a]The Institute of Scientific and Industrial Research (SANKEN), Osaka University, Mihogaoka 8-1, Ibaraki, Osaka 567-0047, Japan
[b]Department of Chemistry, Graduate School of Science, Kobe University, Hyogo Prefecture 657-0013, Japan, and Science and Technology Agency (JST), 4-1-8 Honcho Kawaguchi, Saitama 332-0012, Japan

1. Material synthesis

Preparation of MoS_2 Nanosheets. The lithium intercalation was carried out in a nitrogen-filled glovebox ($[O_2] < 100$ ppm). About 300 mg of bulk MoS_2 (Sigma-Aldrich) was immersed in 3 mL of *n*-butylithium and stirred for 2 days. The stock solution was filtered and washed with 100 mL hexane. Then the semi-dry powder was added in 300 mL of Milli-Q water and ultrasonicated for 1 h. The mixture was centrifugated and washed with Milli-Q water to remove the lithium cation and unexfoliated MoS_2.[S1,S2] It was eventually collected and redispersed in Milli-Q water (pH $\approx$ 6.5). The concentration of MoS_2 in the suspension was determined by inductively coupled plasma (ICP) analysis.

Preparation of Cubic-like TiO_2 Mesocrystals (TMCs). The cubic-like TMCs were synthesized according to references with some modification.[S3,S4] The samples were prepared from precursor solutions containing TiF_4 (Sigma-Aldrich), NH_4NO_3 (Wako Pure Chemical Industries), and H_2O. The TiF_4:NH_4NO_3:H_2O molar ratios were 1:4.9:347. The precursor solutions were placed on a silicon wafer to form a thin layer; the temperature was raised at a rate of 10 °C min^{-1}, and the products were calcined at

500 °C for 2 h. The obtained powders were then calcined at 500 °C in an oxygen atmosphere for 8 h to remove surface residues, including fluorine species, completely (confirmed by X-ray photoelectron spectroscopy (XPS)).

Preparation of TMCs Assembled with MoS_2. The preparation method of the MoS_2/TMC composites was described as follows. 2.6 mg TMCs were impregnated with different concentrations of chemically exfoliated MoS_2 nanosheets in 0.7 mL Milli-Q water (pH ≈ 6.5). After sonication, the suspension was dropped on a silicon wafer and annealed for 10 min on an electric heater in the glovebox ($[O_2] < 100$ ppm). Finally, the product was collected after cooling to room temperature. For the preparation of other reference samples, the same modification procedures were applied for crashed TMCs, P25 (Japan Aerosil), sheet-like TMCs,[S3] and Al_2O_3 nanoparticles (Aldrich; particle size is < 50 nm).

Preparation of Pt Nanoparticle-Loaded TMC (Pt/TMC). Pt/TMC was synthesized according to the literature procedure.[S5] TMCs were stirred in water with H_2PtCl_6 (Aldrich) at room temperature and evaporated the water at 100 °C, and calcined in air at 500 °C. The amount of Pt was 10 wt%, which was determined by ICP.

2. Characterizations. The structures of the samples were examined using X-ray diffraction (XRD; Rigaku, Smartlab; operated at 40 kV and 200 mA, Cu Kα source). The morphologies were investigated using field-emission scanning electron microscopy (FESEM) equipped with EDX analyzer (JEOL, JSM-6330FT) and transmission electron microscopy (TEM) equipped with EDX analyzer (JEOL, JEM 3000F operated at 300 kV or JEM-2100 operated at 200 kV). Scanning TEM (STEM) and energy dispersive spectroscopy (EDS) mapping were performed using a Cs-corrected JEM-ARM200F microscope operated at 200 kV. The Brunauer–Emmett–Teller (BET) surface areas were measured using nitrogen sorption (BEL Japan, BEL-SORP max). The pore volumes and pore diameter distributions were derived from the adsorption isotherms using the Barrett–Joyner–Halenda (BJH) model. The steady-state UV-Vis absorption and diffuse reflectance spectra were measured by UV-Vis-NIR spectrophotometers (Shimadzu, UV-3100 or Jasco, V-570) at room temperature.

The concentration of MoS_2 was determined by ICP (Shimadzu, ICPS-8100). The XPS spectral measurements were performed with the PHI X-tool (ULVAC-PHI).

3. Photocatalytic H_2 Generation Tests. The catalyst of MoS_2/TMC (1 mg) was suspended in 2 mL water with lactic acid (10 vol%) in 10 mL quartz cell and the suspension was shaken for 10 min. Then, the cell was sealed with a rubber septum and purged with Ar gas for 20 min before initiating the irradiation. The sample was irradiated with a UV-LED source (Asahi Spectra, POT-365; 100 mW cm^{-2}) with constant magnetic stirring at room temperature. After the reaction, 0.1 mL of gas was collected from the headspace of the reactor and analyzed using a Shimadzu GC-8A gas chromatograph equipped with an MS-5A column and a thermal conductivity detector. The apparent quantum efficiency (AQE) for hydrogen evolution at each centered wavelength of the monochromatic light with width of ± 5 nm (Asahi Spectra, HAL-320; 0.7 mW cm^{-2}) was calculated via the following equation: AQE = (2 × number of number of hydrogen molecules / number of incident photons) × 100%.

4. Time-Resolved Diffuse Reflectance Measurements. The femtosecond diffuse reflectance spectra were measured by the pump and probe method using a regeneratively amplified titanium sapphire laser (Spectra-Physics, Spitfire Pro F, 1 kHz) pumped by a Nd:YLF laser (Spectra-Physics, Empower 15). The seed pulse was generated by a titanium sapphire laser (Spectra-Physics, Mai Tai VFSJW; fwhm 80 fs). The fourth harmonic generation (330 nm, 3 mJ $pulse^{-1}$) of the optical parametric amplifier (Spectra-Physics, OPA-800CF-1) was used as the excitation pulse. A white light continuum pulse, which was generated by focusing the residual of the fundamental light on a sapphire crystal after the computer controlled optical delay, was divided into two parts and used as the probe and the reference lights, of which the latter was used to compensate the laser fluctuation. Both probe and reference lights were directed to the sample powder coated on the glass substrate, and the reflected lights were detected by a linear InGaAs array detector equipped with the polychromator (Solar, MS3504). The pump pulse was chopped by the mechanical chopper synchronized to one-half of the laser repetition rate, resulting in a pair of spectra with and without the pump, from which the absorption change (% Abs) induced by the pump pulse was estimated. All measurements were carried out at room temperature.

5. Supplementary Calculation on the Coverage of MoS_2 Nanosheets on the External Surfaces of TMCs.

(1) Calculation on the external surface area of TMCs.

$m_{particle} = V_{TiO_2} \times \rho_{anatase}$， $N_{total} = m_{total}^{TiO_2} / m_{particle}$， $S_{total}^{ex} = S_{single}^{ex} \times N_{total}$

V_{TiO_2} is the volume of a TMC and calculated from the FESEM data, where the pore volume was neglected.

S_{single}^{ex} is the external area of a TMC and calculated from FESEM data.

L_{TiO_2} is the face-to-face distance between the lateral facets of TMC (Figure S1).

H_{TiO_2} is the face-to-face distance between the basal facets of TMC (Figure S1).

$\rho_{anatase}$ is 3.84 g/cm³, m_{total} is 5.2 mg.

$m_{total}^{TiO_2} = m_{total} \times 90\ \text{wt\%} = 0.5\times10^{-2}$ g

N_{total} is the total number of TMCs in $m_{total}^{TiO_2}$.

$$\begin{aligned} S_{single}^{ex} &= L_{TiO_2}^2 \times 2 + (L_{TiO_2} \times H_{TiO_2}) \times 4 \\ &= (500\ \text{nm} \times 500\ \text{nm}) \times 2 + (500\ \text{nm} \times 220\ \text{nm}) \times 4 \\ &= 9.4 \times 10^5\ \text{nm}^2 \end{aligned}$$

$$\begin{aligned} m_{particle} &= \rho_{anatase} \times V_{TiO_2} = 3.84\ \text{g/cm}^3 \times (500\ \text{nm} \times 500\ \text{nm} \times 220\ \text{nm}) \\ &= 0.2 \times 10^{-12}\ \text{g} \end{aligned}$$

$$\begin{aligned} S_{total}^{ex} &= S_{single}^{ex} \times N_{total} = 9.4 \times 10^5\ \text{nm}^2 \times (m_{total} / m_{particle}) \\ &= 9.4 \times 10^5\ \text{nm}^2 \times (0.5 \times 10^{-2}\ \text{g} / 0.2 \times 10^{-12}\ \text{g}) \\ &= 9.4 \times 10^5\ \text{nm}^2 \times 0.3 \times 10^{11} \\ &= 2.8 \times 10^{16}\ \text{nm}^2 \end{aligned}$$

(2) Calculation on the coverage of MoS_2 ($\rho_{MoS_2} = 5.06$ g/cm^3):

$$m_{total}^{MoS_2} = 10\ \text{wt\%} \times m_{total} = 10\ \text{wt\%} \times 5.2\ \text{mg} = 0.52 \times 10^{-3}\ \text{g}$$

$$V_{MoS_2} = m_{total}^{MoS_2} / \rho_{MoS_2} = 0.52 \times 10^{-3}\ \text{g} / 5.06\ \text{g/cm}^3 = 0.10 \times 10^{18}\ \text{nm}^3$$

$$S_{total}^{ex} = V_{MoS_2} / d_{thickness}^{monolayer} = 0.10 \times 10^{18}\ \text{nm}^3/1.6\ \text{nm} = 6.0 \times 10^{16}\ \text{nm}^2$$

Since only one side of MoS_2 nanosheets is attached on the external surfaces of TMCs,

$$S_{one\,side}^{ex} = S_{total}^{ex} / 2 = 3.0 \times 10^{16}\ \text{nm}^2$$

Coverage (%) $= S_{one\,side}^{ex}\ (MoS_2) / S_{total}^{ex}\ (\text{TMC}) = 3.0 \times 10^{16}\ \text{nm}^2/2.82 \times 10^{16}\ \text{nm}^2$

≈ 106 %

Ideally, the external surfaces of TMCs are totally covered by MoS_2 nanosheets.

6. Supplementary Tables and Figures.

Table S1. Structural Characteristics of the Samples

Sample	Crystalline phase [a]	S_{BET} (m^2/g)	V_p (cm^3/g)	D_p (nm)	Particle size (nm) [b]	(101)/(001)	MoS_2 loading (wt%)
cubic-like TMC	A	62	0.39	25	22	88 %	0
sheet-like TMC	A	63	0.20	10	39	13 %	0
P25	A & R	55	0.21	19	25	–	0
MoS_2	–	1.2	0.03	114	–	–	0
MoS_2/cubic-like TMC	–	43	0.26	24	–	–	10
MoS_2/sheet-like TMC	–	49	0.19	8	–	–	10
MoS_2/P25	–	51	0.5	22	–	–	10

[a] A and R represent anatase and rutile, respectively.

[b] Average size of the samples estimated from the Scherrer equation.

Table S2. Fractions of 1T-MoS_2 and 2H-MoS_2 [a]

Annealing temperature	Fraction of 1T-MoS_2	Fraction of 2H-MoS_2
room temperature	0.60 ± 0.07	0.40 ± 0.07
80 °C	0.14 ± 0.04	0.86 ± 0.04
160 °C	0.08 ± 0.03	0.92 ± 0.03
240 °C	0.05 ± 0.02	0.95 ± 0.02

[a] Calculated from XPS analysis. The fraction of Mo^{6+} species was ignored.

Table S3. Summary of MoS_2-Based Systems in Hydrogen Generation

Sample	Light source[b]	Sacrificial reagent	Activity, mmol g^{-1} h^{-1}	AQE		
				Value	Wavelength (Intensity)	Light source[b]
$Ru(bpy)_3^{2+}$-MoS_2[S6]	Xe_{300W}	ascorbic acid	39		—	
EY-1T MoS_2[S7][a]	Ha_{100W}	TEOA	26		—	
EY-2H MoS_2[S7]	Ha_{100W}	TEOA	0.05		—	
EY-2H MoS_2/GO[S7]	Ha_{100W}	TEOA	0.54		—	
EY-2H MoS_2/NGO[S7]	Ha_{100W}	TEOA	0.83		—	
EY-2H MoS_2/RGO[S7]	Ha_{100W}	TEOA	3.0		—	
EY-2H MoS_2/NGO[S7]	Ha_{100W}	TEOA	10.8		—	
EY-MoS_2/RGO[S8]	Xe_{300W}	TEOA	2.0	24.2%	460 nm (—)	Xe_{300W}
MoS_2/TiO_2/RGO[S9]	Xe_{350W}	ethanol	2.1	9.7%	365 nm (80 mW cm^{-2})	UV-LED
MoS_2/TiO_2-nano[S10]	Xe_{300W}	formic acid	0.07	1%	355 nm (—)	Xe_{300W}
MoS_2/TiO_2-nano[S11]	Xe_{300W}	methanol	0.07		—	
MoS_2/TiO_2-tube[S12]	Xe_{300W}	Na_2S -Na_2SO_3	1.6		—	
MoS/TMCs[c]	UV-LED_{365}	lactic acid	0.55	7.4%	340 nm (0.7 mW cm^{-2})	Xe_{300W}
Pt/TiO_2[S13]	Xe_{350W}	ethanol	16.7		—	
g-C_3N_4/Pt[S14]	Xe_{300W}	TEOA	19.4	26.5%	400 nm (0.5 mW cm^{-2})	Xe_{300W}
CdS/Co_2P[S15]	LED $_{\geq 420}$	mandelic acid	19.4	6.8%	—	—
P_{HIV}/CoP[S16]	Xe_{500W}	TEOA	12.0		—	

[a] EY is eosin Y.

[b] Xe and Ha indicate xenon and halogen lamp, respectively.

[c] This work.

Table S4. Diffusion Lengths and Diffusion Times Estimated from Figure S14

Direction	Diffusion length L_e, nm [a]	Diffusion time τ_e, ns [b]
a	10.5	0.018
c	8.5	0.012
H	110	202
L	250	1042
d	11	0.018

[a] Obtained by SEM and TEM analyses. The diffusion lengths are the radii of the crystals.

[b] Calculated using equation: $\tau_e = L_e^2/6D_e$, where diffusion coefficient D_e is 10^{-2} cm^2 s^{-1} for electron transfer inside a nanoparticle (direction a, c, and d)[S17] or 10^{-4} cm^2 s^{-1} for interparticle electron transfer (direction H and L) (see Figure S14 for crystal structures).[S18]

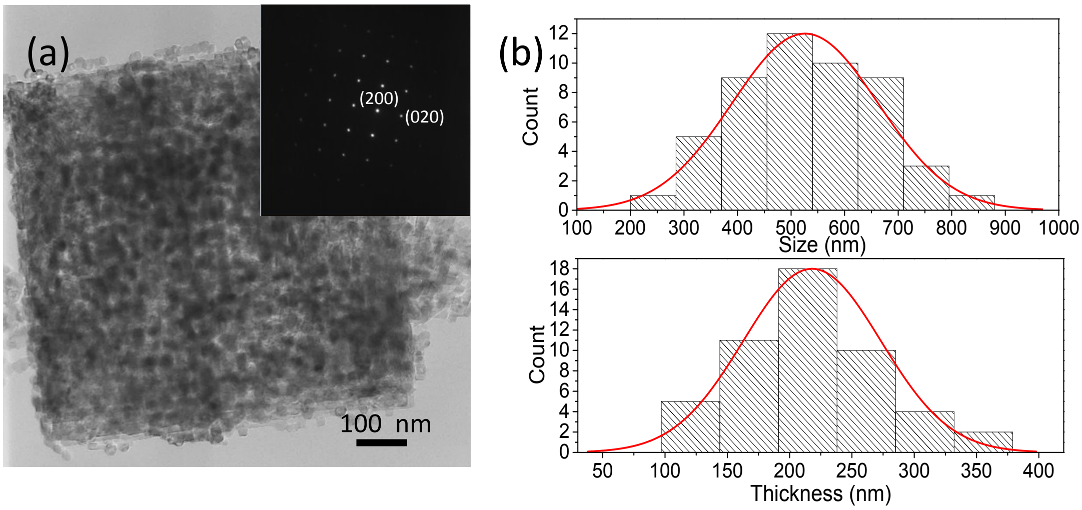

Fig. S1 (a) TEM image of TMC and (b) histogram of size and thickness. The inset in panel (a) is the SAED pattern.

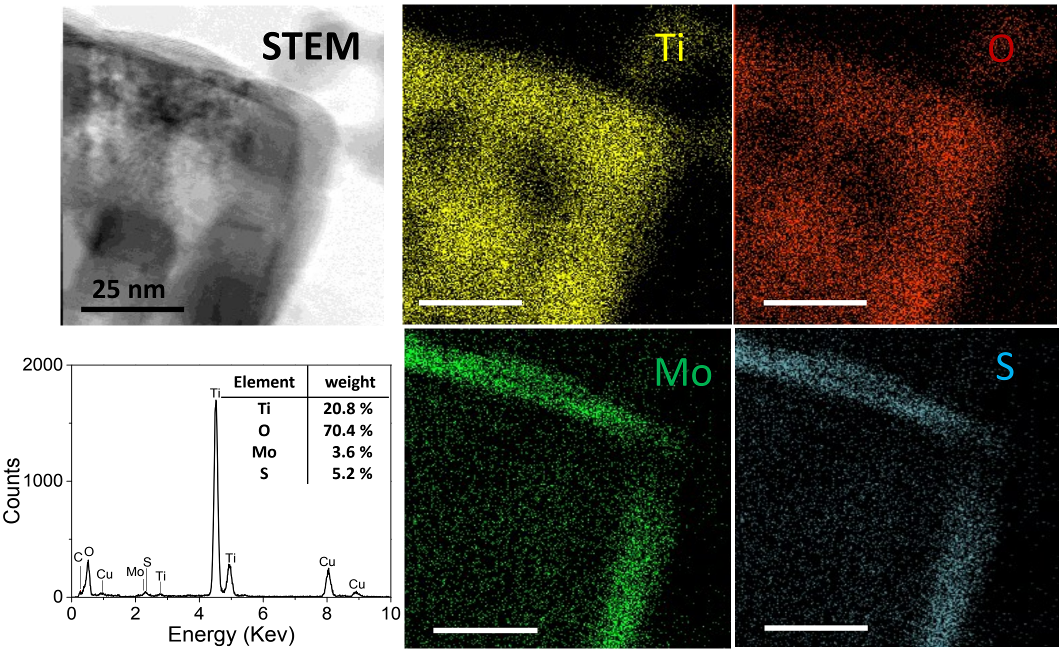

Element	weight
Ti	20.8 %
O	70.4 %
Mo	3.6 %
S	5.2 %

Fig. S2 STEM-EDS elemental mapping images of MoS_2/TMC and EDS analysis. The scale bars in all images represent 25 nm.

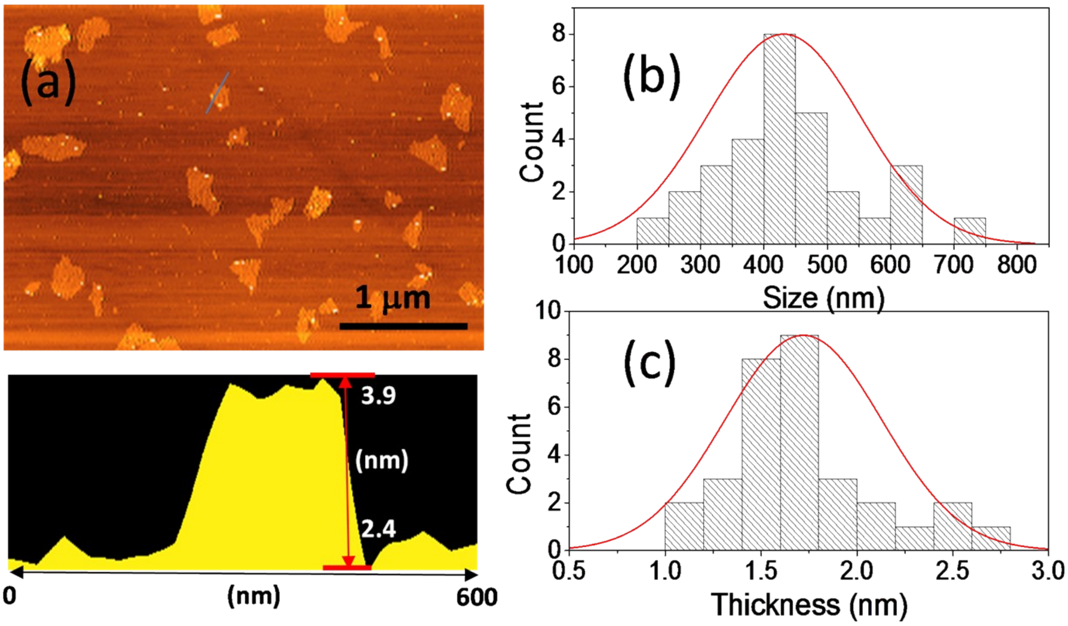

Fig. S3 (a) AFM image of MoS_2 and the histogram of (b) size and (c) thickness.

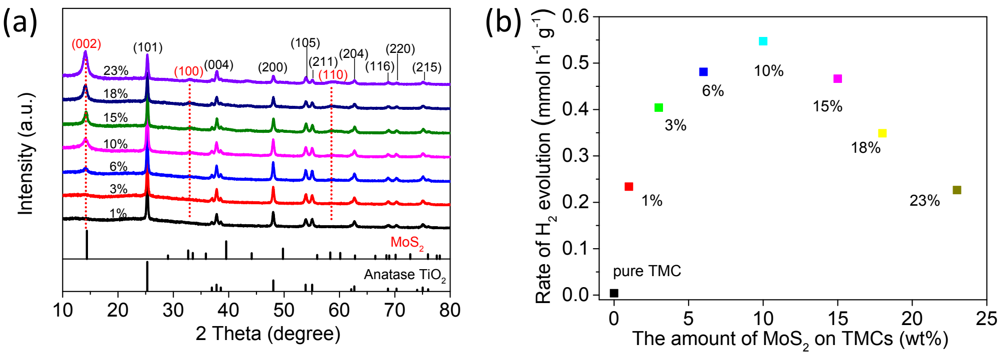

Fig. S4 (a) Powder XRD patterns and (b) the rates of H_2 evolution of TMCs modified with different weights of MoS_2.

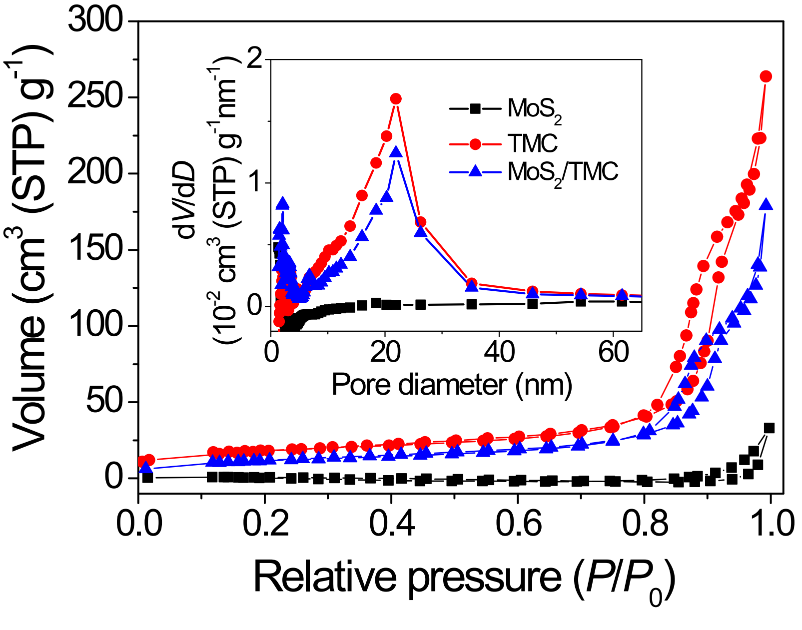

Fig. S5 N_2 adsorption–desorption isotherms and pore size distributions (inset) of MoS_2, TMC, and MoS_2/TMC.

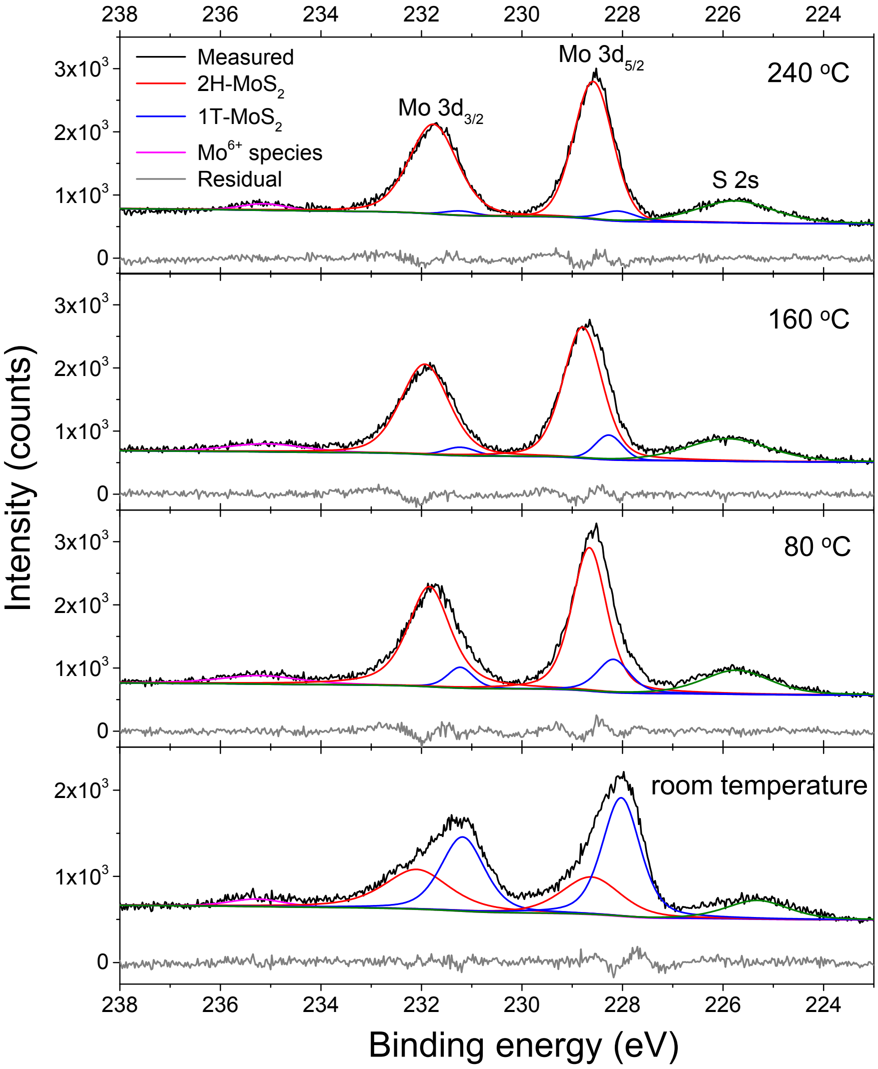

Fig. S6 XPS spectra of Mo 3d from MoS_2/TMC annealed at various temperatures.

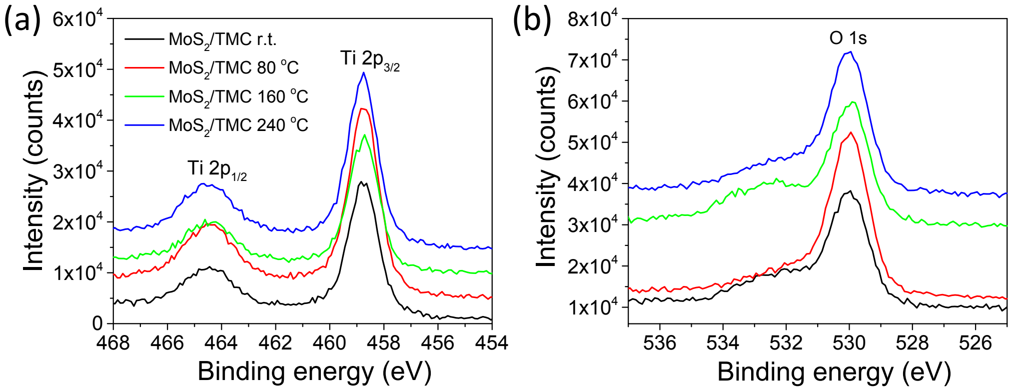

Fig. S7 XPS spectra of Ti 2p and O 1s from MoS_2/TMC annealed at various temperatures.

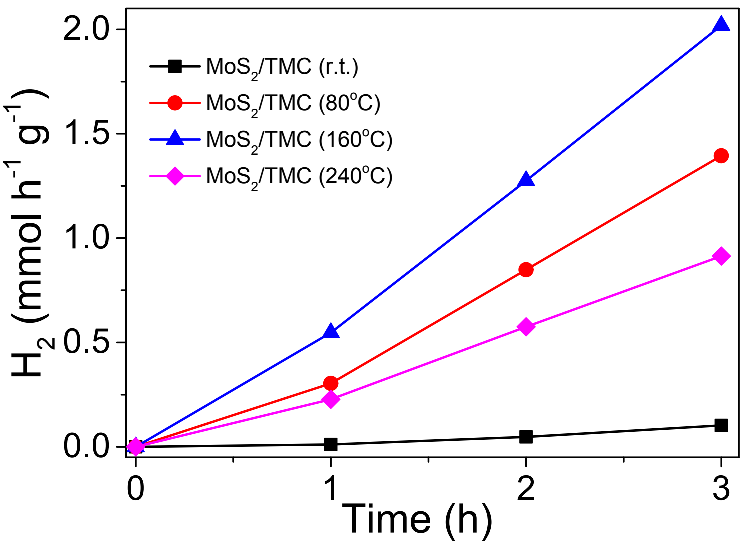

Fig. S8 Hydrogen production activities of the MoS_2/TMC samples annealed at different temperatures.

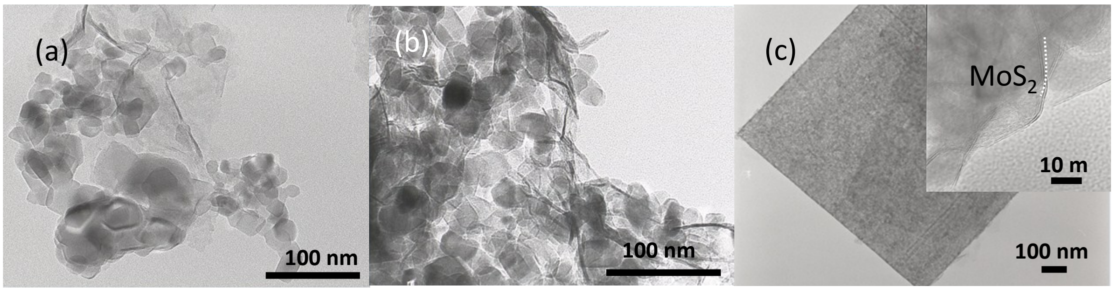

Fig. S9 TEM images of (a) MoS_2/P25, (b) MoS_2/crushed TMC, and (c) MoS_2/sheet-like TMC.

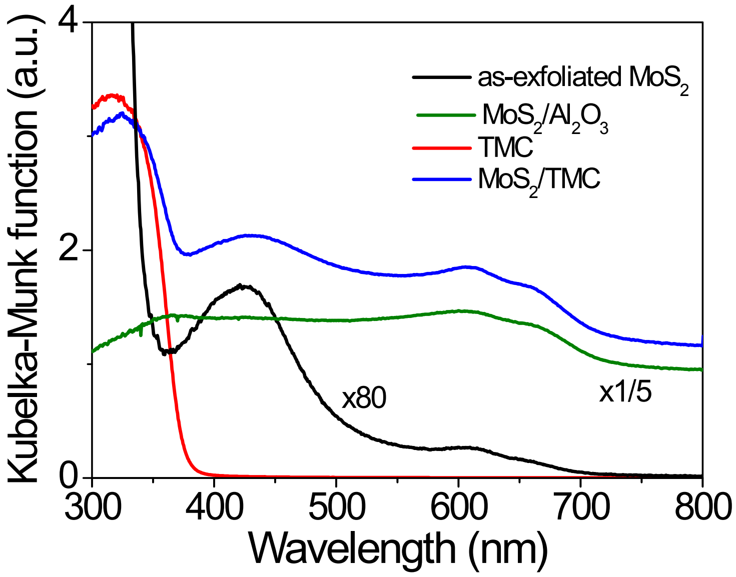

Fig. S10 Steady-state diffuse reflectance spectra of the samples.

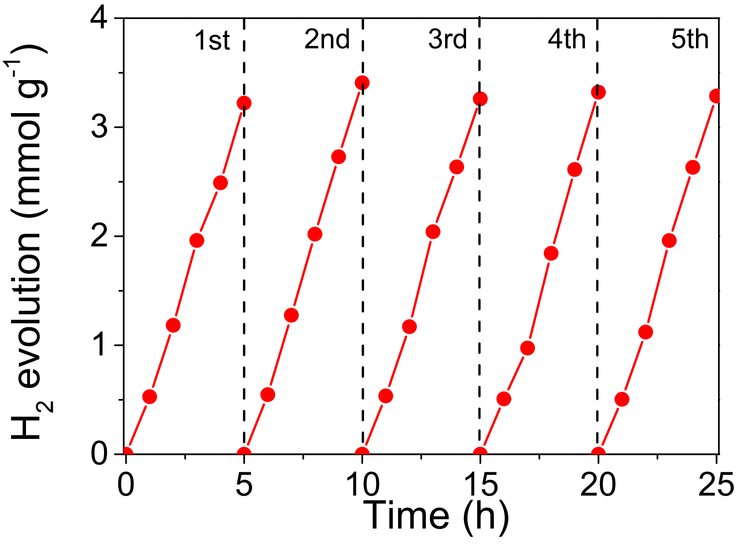

Fig. S11 Repeated runs for H_2 evolution of MoS_2/TMC under UV light irradiation.

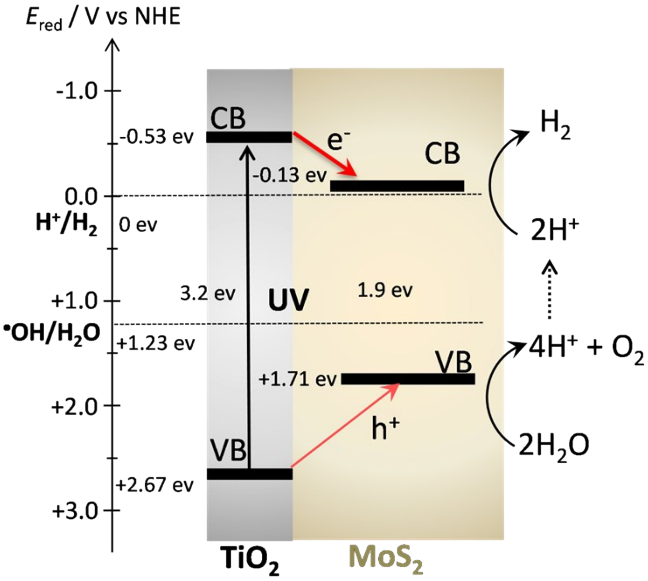

Fig. S12 Schematic illustration of band alignment on MoS_2/TMC.

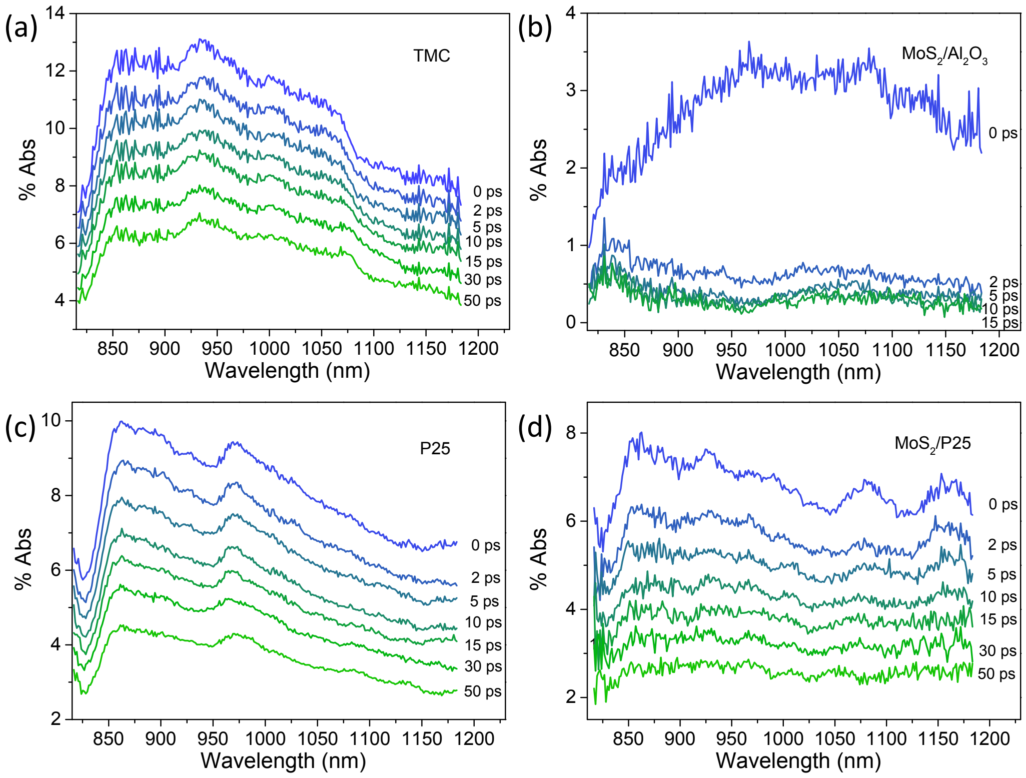

Fig. S13 Time-resolved diffuse reflectance spectra of (a) TMC, (b) MoS_2/Al_2O_3, (c) P25, and (d) MoS_2/P25 after 330 nm flash photolysis.

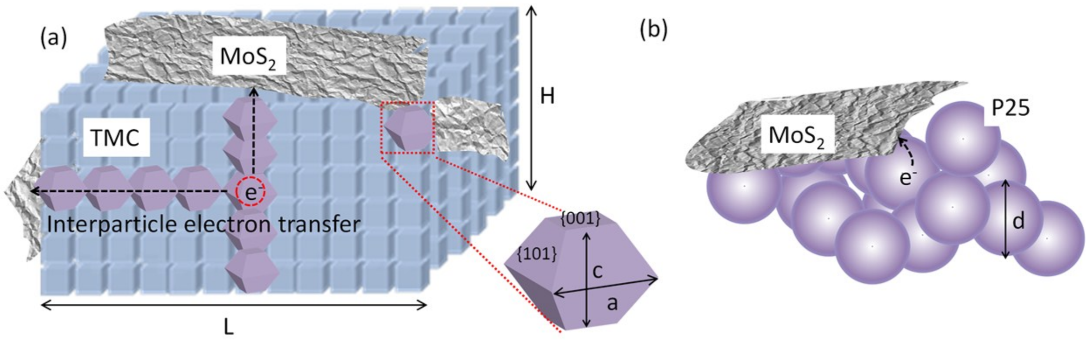

Fig. S14 Models of electron migration processes in (a) MoS$_2$/TMC and (b) MoS$_2$/P25.

References

(S1) G. Eda, H. Yamaguchi, D. Voiry, T. Fujita, M. Chen, M. Chhowalla, *Nano Lett.* 2011, **11**, 5111.

(S2) Yu, Y.; Huang, S. Y.; Li, Y.; Steinmann, S. N.; Yang, W.; Cao, L. *Nano Lett.* 2014, **14**, 553.

(S3) Z. Bian, T. Tachikawa, T. Majima, *J. Phys. Chem. Lett.* 2012, **3**, 1422.

(S4) Z. Bian, T. Tachikawa, P. Zhang, M. Fujitsuka, T. Majima, *J. Am. Chem. Soc.* 2014, **136**, 458-465.

(S5) Z. Bian, T. Tachikawa, W. Kim, W. Choi, T. Majima, *J. Phys. Chem. C* 2012, **116**, 25444.

(S6) X. Zong, Y. Na, F. Wen, G. Ma, J. Yang, D. Wang, Y. Ma, M. Wang, L. Sun, C. Li, *Chem. Commun.* 2009, **30**, 4536.

(S7) U. Maitra, U. Gupta, M. De, R. Datta, A. Govindaraj, C. N. R. Rao, *Angew. Chem., Int. Ed.* 2013, **52**, 13057.

(S8) S. Min, G. Lu, *J. Phys. Chem. C* 2012, **116**, 25415.

(S9) Q. Xiang, J. Yu, M. Jaroniec, *J. Am. Chem. Soc.* 2012, **134**, 6575.

(S10) S. Kanda, T. Akita, M. Fujishima, H. Tada, *J. Colloid Interface Sc.* 2011, **354**, 607.

(S11) Q. Liu, Z. Pu, A. Asiri ,A. H. Qusti, A. O, Al-Youbi, X. Sun, *J Nanopart Res* 2013, **15**, 2057.

(S12) W. Zhou, Z. Yin, Y. Du, X. Huang, Z. Zeng, Z. Fan, H. Liu, J. Wang, H. Zhang, *Small* 2013, **9**, 140.

(S13) J. Yu, L. Qi, M. Jaroniec, *J. Phys. Chem. C* 2010, **114**, 13118.

(S14) D. J. Martin, K. Qiu, S. A. Shevlin, A. D. Handoko, X. Chen, Z. Guo, J. Tang, *Angew. Chem., Int. Ed* 2014, **53**, 9240.

(S15) S. Cao, Y. Chen, C. Hou, X. Lv, W. Fu, *J. Mater. Chem. A* 2015, **3**, 6096.

(S16) J. Tian, N. Cheng, Q. Liu, W. Xing, X. Sun, *Angew. Chem., Int. Ed.* 2015, **541**, 1.

(S17) B. Enright, D. Fitzmaurice, *J. Phys. Chem.* 1996, **100**, 1027.

(S18) S. Nakade, Y. Saito, W. Kubo, T. Kitamura, Y. Wada, S. Yanagida, *J. Phys. Chem. B* 2003, **107**, 8607.